

# Levitation characteristics of a high-temperature superconducting Maglev system for launching space vehicles

Wenjiang Yang<sup>a,\*</sup>, Yu Liu<sup>a</sup>, Xiaodong Chen<sup>a</sup>, Zheng Wen<sup>a</sup>, Yi Duan<sup>a</sup>, Ming Qiu<sup>b</sup>

<sup>a</sup> School of Astronautics, Beijing University of Aeronautics and Astronautics, No. 37 Xueyuan Road, Haidian District, Beijing 100083, PR China

<sup>b</sup> Institute of Electrical Engineering, Chinese Academy of Sciences, Beijing 100080, PR China

Received 9 April 2006; received in revised form 23 January 2007; accepted 30 January 2007

Available online 9 February 2007

## Abstract

Maglev launch assist is viewed as an effective method to reduce the cost of space launch. The primary aerodynamic characteristics of the Maglev launch vehicle and the space vehicle are discussed by analyzing their aerodynamic shapes and testing a scale mode in a standard wind tunnel. After analyzing several popular Maglev systems, we present a no-controlling Maglev system with bulk YBaCuO high-temperature superconductors (HTSs). We tested a HTS Maglev system unit, and obtained the levitation force density of 3.3 N/cm<sup>2</sup> and the lateral force density of 2.0 N/cm<sup>2</sup>. We also fabricated a freely levitated test platform to investigate the levitation characteristics of the HTS Maglev system in load changing processes. We found that the HTS system could provide the strong self-stable levitation performance due to the magnetic flux trapped in superconductors. The HTS Maglev system provided feasibility for application in the launch vehicle. © 2007 Elsevier B.V. All rights reserved.

PACS: 85.25.Ly

Keywords: Magnetic levitation vehicles; High-temperature superconductors; Aerospace ground support; Space flight

## 1. Introduction

Significant reduction in the launch cost is a precondition for the expansion of commercial activities into space. Maglev launch assist vehicle (Maglifter) has been proposed [1–3] to provide a high ground takeoff velocity (up to 1000 km/h), which is expected to cut down the propellant consumption and the structure mass for space vehicles.

On the other hand, Maglev technology has made great progress since the 1920s. The ground velocity of the Maglev train has attained 550 km/h, which provides feasibility for the achievement of Maglifter. However, during the Maglev launch assist, the Maglifter will endure complicated aerodynamic effects, such as aerodynamic forces and moments, which will cause some problems on the

Maglev system. In this article, we firstly investigate the primary aerodynamic properties of the Maglifter, and then provide a design for a HTS Maglev system for the Maglifter and we report on its levitation characteristics as determined by experimental measurements and analyses.

## 2. Aerodynamic analyses

A primary configuration of the Maglifter launching space vehicle is described in Fig. 1. The space vehicle is fixed above the Maglifter by a support structure. The levitation force ( $L_M$ ) is provided between the Maglifter and the guideway to reduce the friction loss. The Maglifter and the space vehicle when exposed to atmosphere will experience aerodynamic effects with increasing assist velocity. In the two-dimensional motion plane, the aerodynamic effects can be resolved into aerodynamic drag force ( $D$ ), lift force ( $L$ ) and pitching moment ( $M$ ), which may be described in the following equations:

\* Corresponding author. Tel.: +86 010 82339444.

E-mail address: [yangwjbuaa@sa.buaa.edu.cn](mailto:yangwjbuaa@sa.buaa.edu.cn) (W. Yang).

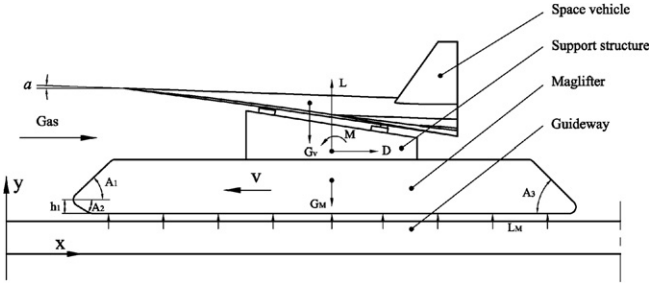


Fig. 1. Sketch map of Maglifter under the aerodynamic effects.



Fig. 2. Scale model of the Maglifter and the space vehicle.

$$D = \frac{1}{2} C_D \rho V^2 S \quad (1)$$

$$L = \frac{1}{2} C_L \rho V^2 S \quad (2)$$

$$M = \frac{1}{2} C_m \rho V^2 S c_A \quad (3)$$

where  $C_D$ ,  $C_L$ ,  $C_m$  are separately aerodynamic drag, lift, and pitching moment coefficients.  $\rho$  is the air density at sea level,  $V$  is the assist velocity,  $S$  is the aerodynamic reference area, and  $c_A$  is the wing mean aerodynamic chord.

$S$  and  $c_A$  are size properties of the Maglifter and the space vehicle.  $C_D$ ,  $C_L$ ,  $C_m$  are the main parameters which decide the aerodynamic properties, and they are strictly related to the aerodynamic shapes of the Maglifter and the space vehicle, the assist velocity  $V$ , and the attack angle  $\alpha$  shown in Fig. 1. In general, reasonable aerodynamic coefficients are obtained by the aerodynamic shapes being designed optimally.

As shown in Fig. 1, a typical aerodynamic shape of the waverider is used for the space vehicle, which can provide a high  $C_L$ - $C_D$  ratio for takeoff of the space vehicle. A typical aerodynamic shape of the Maglev train is used in the Maglifter, which can provide a low  $C_L$ - $C_D$  ratio for reducing the drag force and the lift force of the Maglifter. In Fig. 1,  $A_1$ ,  $A_2$ ,  $A_3$ , and  $h_1$  are four main parameters which affect the aerodynamic shape of the Maglifter. A group of optimal values of the parameters were obtained by means of a computation fluid dynamics (CFD) method [4]. These values were  $20^\circ$ ,  $0^\circ$ ,  $40^\circ$ , and  $0$  m, respectively. In order to analyze the effectiveness of the method and obtain more accurate aerodynamic characteristics, we manufactured an approximately 1/59 scale model of the Maglifter and the space vehicle, as shown in Fig. 2, and then tested the model in the FD-06 wind tunnel at the China Academy of Aerospace Aerodynamics (CAAA). The experimental values for the aerodynamic coefficients are shown in Figs. 3 and 4.

As shown in Figs. 3 and 4, the total drag, lift, and pitching moment coefficients increase with the assist velocity. The increment of the lift force coefficient is believed to be related to the waverider shape of the space vehicle. According to Eqs. (1)–(3), the total drag force, lift force, and pitching moment increase as a quadratic function of the velocity. The aerodynamic lift force will increase the levita-

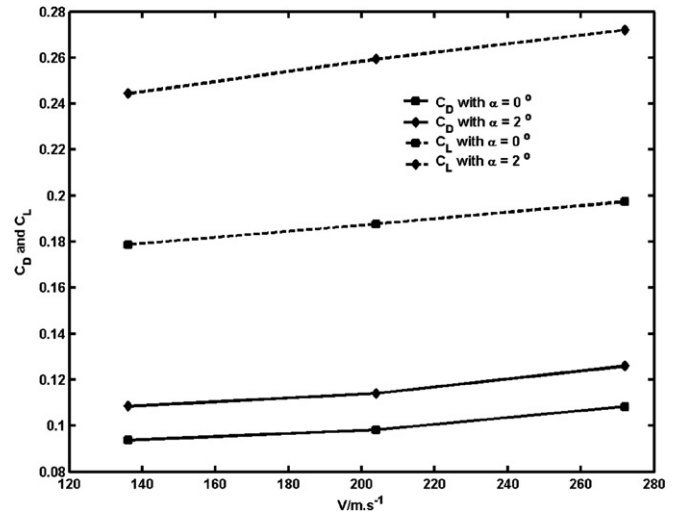


Fig. 3. Aerodynamic drag and lift coefficients.

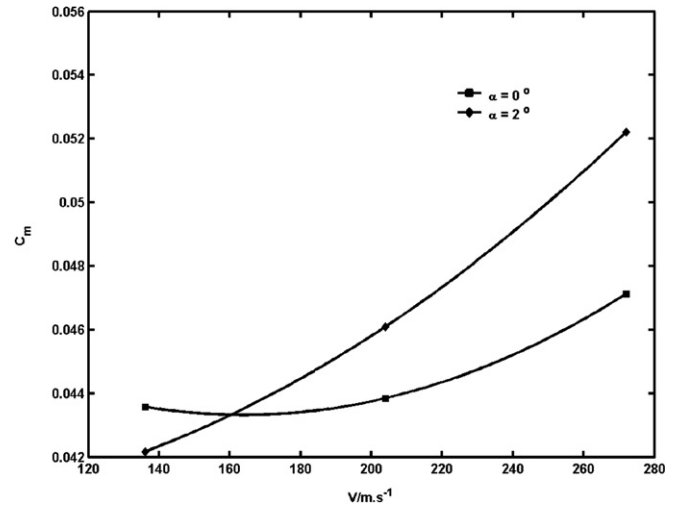


Fig. 4. Aerodynamic pitch moment coefficients.

tion gap, and the pitching moment will affect the pitch equilibrium of the Maglifter. Therefore, it is desirable to present a kind of Maglev system that can restrain this influence.

### 3. Maglev system consideration

The electromagnetic suspension (EMS) system and the electrodynamic suspension (EDS) system are two popular Maglev systems proposed in the last century [5]. The EMS system works on the basis of magnetic attraction, which is an active suspension system and requires complicated control technologies. The EDS system is a passive repulsion system and has a perfect levitation gap above 100 mm. However, the superconductors in the EDS system need to operate in liquid helium employing expensive and complicated low temperature technologies. Also, no-levitation at low velocity and instabilities at high velocity also cause some problems.

The Maglifter is expected to provide a sufficiently high takeoff velocity for space vehicles in a short time. Furthermore, the aerodynamic effects lead to a complex working environment on the Maglev system. Especially, the levitated weight can approach zero due to the increasing aerodynamic lift force. The EMS system and the EDS system have difficulties in controlling the upward levitation vehicle only by the attraction force or the repulsive force.

The levitation of permanent magnets (PMs) over bulk HTS magnets and its applications in a Maglev system have been investigated for the last 20 years [6–9]. Based on high critical current density and strong flux pinning in superconductors, HTS Maglev systems can produce strong repulsion forces, attraction forces, and lateral restoring forces, and these forces can cause a self-stable levitation system both in the vertical and lateral directions. Therefore, the HTS Maglev system provides an attractive approach for the Maglifter.

In order to investigate the feasibility of the HTS system, as shown in Fig. 5, we present a sketch of a PM-HTS Maglev system unit. It consists of a cryostat with bulk YBaCuO superconductors and a PM guideway. The superconductors are about 30 mm in diameter and 18 mm in thickness, and are fixed firmly on the inside bottom of the cryostat with vacuum structure. The cryostat is cooled with liquid nitrogen to provide a long-time 77 K temperature. To achieve an effective levitation clearance, the bottom thickness of the cryostat is designed to be 5 mm.

The PM guideway is a flux-collecting structure composed of a stack of PMs and iron shims. The high magnetic

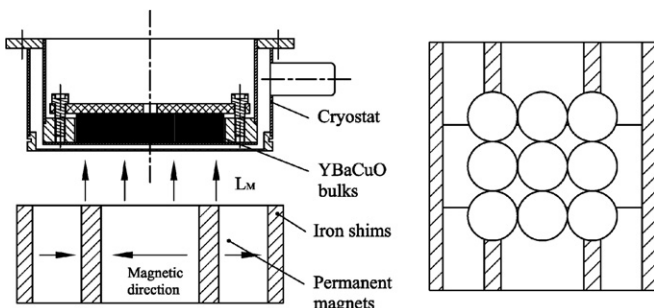


Fig. 5. Sketch map of a PM-HTS bulks suspension system.

field distribution is concentrated over the middle iron shims. The PM guideway was designed optimally by calculating the influence of the sizes of the PMs and iron shims on the magnetic field distribution [10]. Finally, the magnetic field value was raised to 1.5 T on the top surface of iron shims. The high magnetic field gradient was produced in the vertical direction of the guideway, which leads to the large levitation force. The magnetic field is inhomogeneous along the width direction of the guideway, which provides the lateral stability of the Maglev system.

As shown in Figs. 5 and 9 YBaCuO bulks are positioned in a proposed arrangement relative to the PM guideway. Because the levitation characteristics depend on the magnetization process of bulk superconductors [7], we investigated the levitation and guidance forces of the arrangement at different field cooling heights (FCHs). The height is the distance of the YBaCuO bulks above the surface of the PM guideway, which produces different magnetic field distributions at different FCHs. The arrangement was cooled, respectively at FCH = 100 mm, 35 mm, and 25 mm, and then was moved vertically to a distance of 15 mm, and from there on to a distance of 100 mm, before finally being returned to the start point. During each cycle, the levitation force of the arrangement acting on the guideway was measured and is shown in Fig. 6.

It can be seen that the levitation forces vary approximately as the negative exponential of the vertical distance, and the maximum force is up to 267 N and 3.3 N/cm<sup>2</sup> at a distance of 15 mm. The forces are highly hysteretic, indicating that there are two levitated equilibrium positions for a given levitated weight in the descending and ascending processes. The FCH has a direct effect on the levitation force. The higher FCH leads to the larger levitation force. The attractive force increases with decreasing of the FCH. The hysteretic properties and the influence of FCHs are believed to be related to the flux pinning mechanisms in

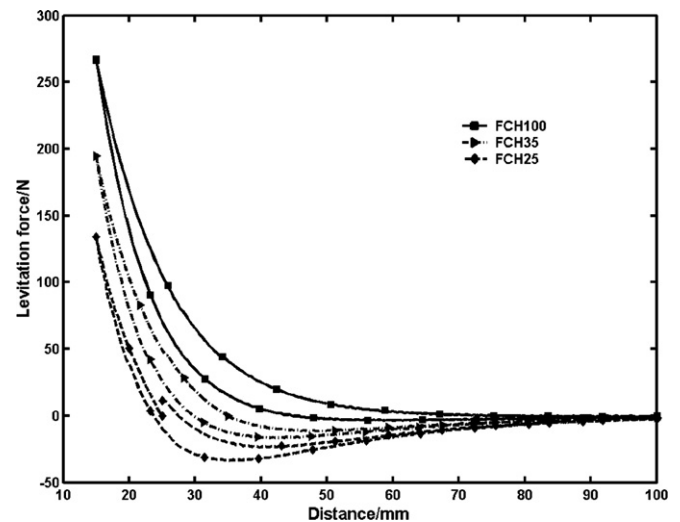


Fig. 6. Levitation force vs. vertical distance for various FCHs.

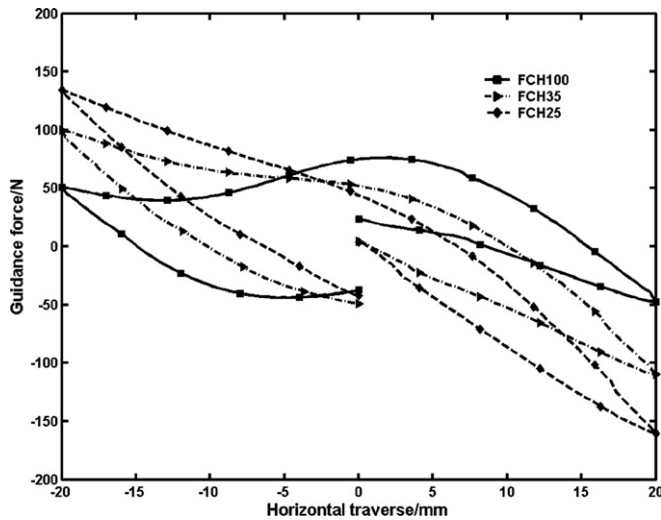


Fig. 7. Guidance force vs. horizontal traverse for various FCHs.

superconductors [11], which cause more magnetic flux to be trapped in the superconductors with decreasing of the FCH and the vertical distance.

The guidance forces of the arrangement were also measured at the various FCHs. When the arrangement was cooled at a given FCH, it was moved vertically to a measuring height of 15 mm, and then the guidance forces were measured in several horizontal traverses of 20 mm. The results are shown in Fig. 7. It can be seen that the guidance force increases with the horizontal traverse to resist the lateral movement, and the maximum force in FCH = 25 mm is up to 160 N and 2.0 N/cm<sup>2</sup> at the traverse of 20 mm. The forces are also highly hysteretic and increase with decreasing FCH. It is believed that more magnetic flux is trapped in superconductors at low FCH, which provides the stronger lateral stability.

#### 4. PM-HTS Maglev test platform

Based on the design and measurements of the Maglev system unit, a demo PM-HTS Maglev test platform was built and is shown in Fig. 8. It mainly consists of PM tracks, HTS units, adjusting equipment for the FCH, measuring equipment for the levitation characteristics, and a flat structure connected to all these equipment items.

Double PM tracks were constructed symmetrically on a concrete foundation. A HTS unit was composed of a cryostat and nine HTS bulks. Six HTS units were fixed to the bottom of the flat structure. The adjusting equipment for the FCH was driven by two sets of stepping-motors to change the FCH of the test platform. After the HTS units are cooled at some height, the adjusting equipment descends to make the test platform levitate freely over the PM tracks. The levitation properties of the test platform were measured by four difference sensors and quantitative poises. The difference sensors were positioned vertically on the four corners of the flat structure. When different

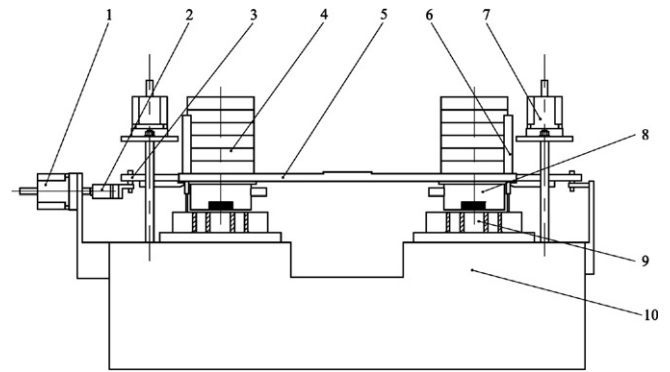


Fig. 8. Sketch map of a demo PM-HTS Maglev test platform: (1) stepping motor, (2) force transducer, (3) dowel structures, (4) poises, (5) flat structure, (6) difference sensors, (7) adjusting equipment for FCHs, (8) HTS units, (9) PM tracks, and (10) foundation.

amounts of poises were loaded on the flat structure, the sensors measured the levitation gaps between the bottom of the cryostats and the surface of the tracks. The guidance force of the test platform was measured by a force transducer, which was joined horizontally to the flat structure by means of dowel structures. The force transducer was moved by a stepping motor to cause the lateral movement of the test platform.

In order to investigate the load performance of the test platform, the platform was measured in three continuous loading/unloading cycles. The FCH was set at 35 mm. The initial mass of the test platform was 45 kg. During each cycle, poises were loaded uniformly on the test platform, in turn from 0 kg to 100 kg and then were unloaded in turn from 100 kg to 0 kg. The difference sensors measured the levitation gaps as each load was changed. The data curves are shown in Fig. 9.

It can be seen that the levitation gap in the first loading/unloading cycle shows a large hysteresis loop, which is sim-

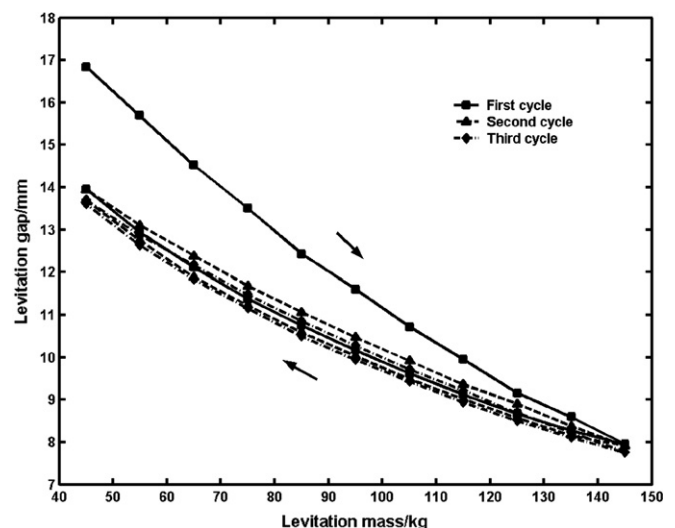


Fig. 9. Levitation gaps in continuous loading/unloading cycles.

ilar to the phenomena shown in Fig. 6, suggesting that the penetration and pinning of flux lines in the superconductors led to energy loss in the first loading process. In the second or the third cycle, the difference of the levitation gaps in the loading and unloading processes appears to approach to zero, suggesting a slight energy loss, and the trapped magnetic flux in the superconductors reaches equilibrium. Therefore, the HTS system can achieve stable levitation performance in the load changing processes, except for the initial one.

When the measurements of the levitation characteristics were completed, the guidance forces of the test platform were measured for three continuous unloading conditions. The initial load condition was 100 kg, then 60 kg, and finally to 0 kg. The guidance force was measured as each load was changed. The data curves are shown in Fig. 10.

As shown in Fig. 9, the levitation gap is increased from 8 mm to 14 mm when the load is changed from 100 kg to 0 kg. However, Fig. 10 shows that the guidance forces in the unloading conditions decrease a small amount, which indicates that the trapped magnetic flux in the superconductors changed little with the increase of the levitation gap. The trapped flux played an important role in causing the lateral stability of the HTS system.

In order to investigate experimentally the influence of the pitching moment on the levitation characteristics, the poises were loaded on one side of the test platform to produce a pitching moment. The poises were loaded in turn from 0 kg to 40 kg and then were unloaded in turn from 40 kg to 0 kg. The levitation gap for the loading side and the one for the no-loading side are both shown in Fig. 11. It can be seen that the levitation gap for the loading side decreases as the unbalanced load is increased, and the one for the no-loading side behaves oppositely. When the unbalanced load is unloaded, the levitation gaps on both sides return to the initial value with a difference of less than 1 mm, indicating the levitation characteristics of the

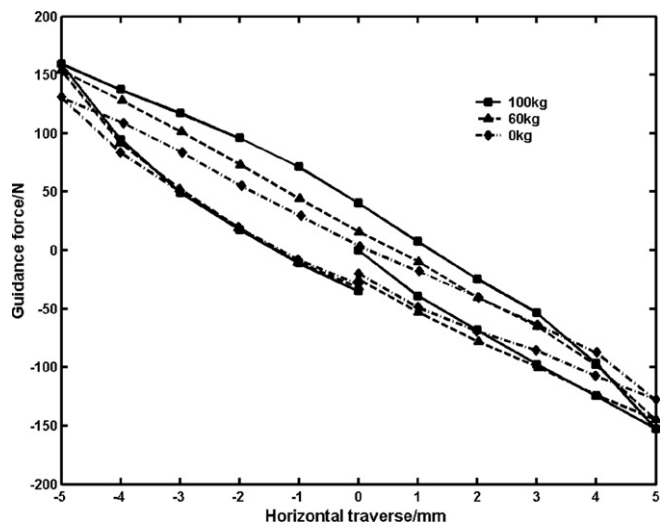


Fig. 10. Guidance force for three continuous unloading conditions.

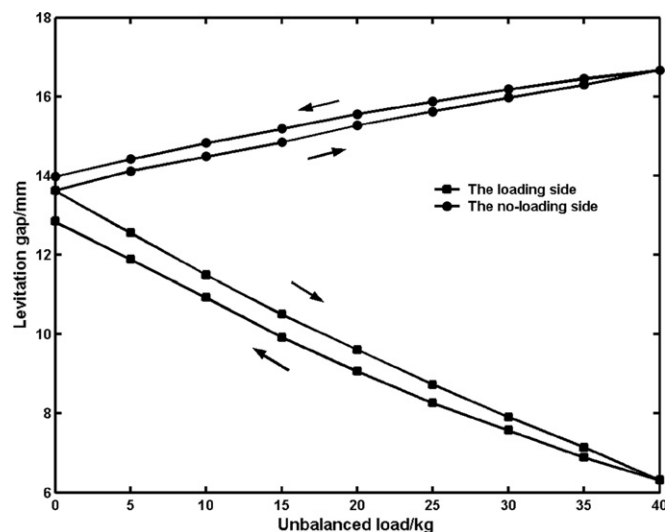


Fig. 11. Influence of unbalanced loads on the levitation gaps.

test platform under the pitching moment show nearly reversible levitation behavior.

During the Maglev launch assist, the aerodynamic lift force and pitching moment will increase with the assist velocity. The levitation gap of the Maglifter and the inhomogeneity of the levitation gap will be increased. According to the experimental data shown in Figs. 9–11, due to the trapped magnetic flux in the superconductors, stability is reached after the initial loading process and the HTS Maglev system can provide stable levitation characteristics in the upward direction.

## 5. Summary

We investigated the primary aerodynamic characteristics of the Maglifter and the space vehicle by analyzing their aerodynamic shapes and testing a designed scale mode in a standard FD-06 wind tunnel. We found that the total aerodynamic drag force, lift force, and pitching moment increase as a quadratic function of the assist velocity. In order to reduce the controlling difficulties in the Maglev launch assist, we selected a self-stable HTS Maglev system and presented a sketch of the PM-HTS part of the system. The system consisted of a cryostat with a bottom thickness of 5 mm and a flux-collecting PM guideway. The Maglev system unit was measured at large repulsive force, attractive force and lateral force, and its levitation characteristics were found to be strongly dependent on the FCH. We also fabricated a freely levitated test platform which consisted of six Maglev units. We observed that the levitation and guidance properties of the test platform were stable during load changing processes. It is believed that the levitation characteristics are closely related to the trapped magnetic flux in the superconductors. The increment and stabilization of the magnetic flux should contribute to a strong self-stable levitation system for the Maglifter.

## Acknowledgement

This work was supported by the innovation foundation of Beijing University of Aeronautics and Astronautics (BUAA) for Ph.D. graduates.

## References

- [1] J.H. Schultz, A. Radovinsky, R.J. Thome, B. Smith, J.V. Minervini, R.L. Myatt, R. Meinke, M. Senti, *IEEE Trans. Appl. Supercon.* 11 (1) (2001) 1749.
- [2] A.J. William, *IEEE Trans. Magn.* 37 (1) (2001) 55.
- [3] W.J. Yang, Y. Liu, B. Yang, *J. Beijing Univ. Aeronaut. Astronaut.* 31 (2005) 105.
- [4] Y. Liu, W.J. Yang, Y. Duan, X.D. Chen, *J. Beijing Univ. Aeronaut. Astronaut.* 32 (2006) 1180.
- [5] Hyung-Woo Lee, Ki-Chan Kim, Ju Lee, *IEEE Trans. Magn.* 42 (7) (2006) 1917.
- [6] F. Hellman, E.M. Gyorgy, D.W. Johnson Jr., H.M. O' Bryan, R.C. Sherwood, *J. Appl. Phys.* 63 (2) (1988) 447.
- [7] J.R. Hull, A. Cansiz, *J. Appl. Phys.* 86 (1999) 6396.
- [8] N. Koshizuka et al., *Physica C* 386 (2003) 444.
- [9] H. Fujimoto, H. Kamijo, *Physica C* 341–348 (2000) 2529.
- [10] M. Qiu, W.J. Yang, Z. Wen, L.Z. Lin, G.H. Yang, Y. Liu, *IEEE Trans. Appl. Supercon.* 16 (2) (2006) 1120.
- [11] F.C. Moon, M.M. Yanoviak, R. Ware, *Appl. Phys. Lett.* 52 (18) (1988) 1534.